Monatshefte für Chemie 132, 83–95 (2001)

Monatshefte für Chemie
Chemical Monthly

Printed in Austria

Thin Film Counterelectrodes with High Li Charge Capacity for Electrochromic Windows

Franco Varsano[1], **Francesca Decker**[1,*], and **Enrico Masetti**[2]

[1] Chemistry Department, University of Roma “La Sapienza”, I-00185 Roma, Italy
[2] Thin Film Optics Laboratory, ENEA-La Casaccia, I-00060 Roma, Italy

Summary. Ce-V mixed oxide films have been deposited by RF sputtering with the aim of increasing the Li charge capacity of counter electrodes in smart windows. Such mixed oxides have shown high transmittance and optical passivity in the visible region. After electrode pre-conditioning by cyclic voltammetry, a good electrochemical reversibility in $LiClO_4$ – propylene carbonate electrolyte was observed, and large Li-charge capacity under galvanostatic charging (up to $50\,mC \cdot cm^{-2}$) has been measured. The electrode charge capacity decreased after prolonged insertion-deinsertion cycles, whereas the photoptic transmittance remained about constant. After 800 cycles the Li-charge capacity decreased to $40\,mC \cdot cm^{-2}$. The Li diffusion coefficient inside the films measured by electrochemical impedance and by galvanostatic titration ranged from $10^{-11}\,cm^2 \cdot s^{-1}$ to $10^{-13}\,cm^2 \cdot s^{-1}$. We observed that the Li charge capacity of the film electrodes is a function of the film deposition conditions, because it increased with the vanadium oxide concentration in the target and with the oxygen content in the sputtering atmosphere.

Keywords. Electrochromism; Mixed oxides; Vanadates, RF sputtering; Li diffusion coefficient.

Introduction

Optically passive counterelectrodes for smart windows require ion-storage materials with large charge capacity and high transparency both in the oxidized and in the reduced state [1]. So far, such favourable properties have never been reached by a single, stoichiometric compound. Cerium oxide, for example, has very good optical properties, but its charge capacity is rather low as is its lithium diffusion coefficient [2]. Ce-based oxide films, like CeO_2/TiO_2 films [3, 4], exhibit a characteristic high transparency associated with a reasonable ion-storage capacity and optical passiveness with respect to charging/discharging reactions. In comparison with Ti oxide, V oxide films have the advantage of very large charge capacities (30–$40\,mC \cdot cm^{-2}$), but the disadvantage of a strong residual yellow color [5]. The quenching of this color has been pursued in recent years by means of appropriate mixtures of Ce/V, Ti/V [6], Nb/V, and Cr/V oxides [7]. The first two mixed oxides turned out to be extremely promising materials. Ceria-vanadia represents, in fact, a new class of optically passive counterelectrodes with good properties for use as counter-

---

[*] Corresponding author

electrodes in an electrochromic (EC) window [8, 9]. Such materials, when prepared as thin films by sol-gel deposition on conductive glass, are transparent and have a good capacity (around $20\,\mathrm{mC \cdot cm^{-2}}$). An appropriate synthesis of uniform and homogeneous thin films of this Ce orthovanadate *via* the sol-gel route has been developed by *Orel et al.* [10]. However, in order to darken completely a film of WO_3 of a thickness of 250 nm, an inserted charge of at least $30\,\mathrm{mC \cdot cm^{-2}}$ is necessary [11].

In a first effort to produce a counterelectrode material with high Li charge capacity by RF sputtering (a deposition technique more suitable than sol-gel for coating large-area glazings) we obtained ceria-vanadia films in which up to $60\,\mathrm{mC \cdot cm^{-2}}$ were exchanged upon the first few galvanostatic cycles [12]. The material bandgap energy was 2.6 eV, which is lower than the bandgap of cerium oxide and of stoichiometric $CeVO_4$ (an orthovanadate also known as wakefieldite [13]; 3.1–3.3 eV), but larger than the bandgap of pure V_2O_5 (2.2 eV). Such sputtered material is therefore almost transparent in the visible region. The preliminary cyclic voltammetries have shown a promising Li ion intercalation capacity which was preserved during subsequent cycles. The above favourable properties prompted us to continue related investigations and to check if the large charge capacity of vanadium oxides and the excellent stability of Ce oxides would be preserved in the sputtered mixed oxide. Sputtered films of mixed oxides of controlled thickness and composition, which are likely to support high intercalation rates, can be deposited by using targets made of pressed oxide powders to cut down costs associated to process development. We observed that the ratios of metals in the sputtered films, in fact, approached closely those of the mixed oxide targets. This strategy appeared particularly indicated to develop new materials that can be quickly prepared with conventional laboratory facilities.

The aim of this work, therefore, has been to develop ceria-vanadia sputtered films controlling the preparation conditions in order to reproduce and to improve the favourable properties of similar films obtained previously by the sol-gel process. Among the electrochemical properties of such passive counterelectrodes, we have tried to improve the film charge capacity and the Li ion insertion rate. These two parameters determine the optical contrast and the time response of the electrochromic window, two of the most important properties of the device.

Results and Discussion

Intercalation properties of thin films

The electrodes prepared with the two different Ce/V-oxide targets showed comparable electrochemical behavior as can be seen from their cyclic voltammograms (CV) in Figs. 1a and 1b. From the vanadium-rich target, films with a higher V/Ce ratio resulted; this, in turn, allowed for a larger Li ion charge capacity of this electrode. The shape of the CVs denotes larger currents for the V-rich electrode and a sharp negative peak at 1.7 V.

The presence of oxygen in the sputtering atmosphere favoured the growth of thin film electrodes with some crystalline structure and with a CV more similar to that of the stoichiometric $CeVO_4$ (wakefieldite) obtained by the sol-gel technique

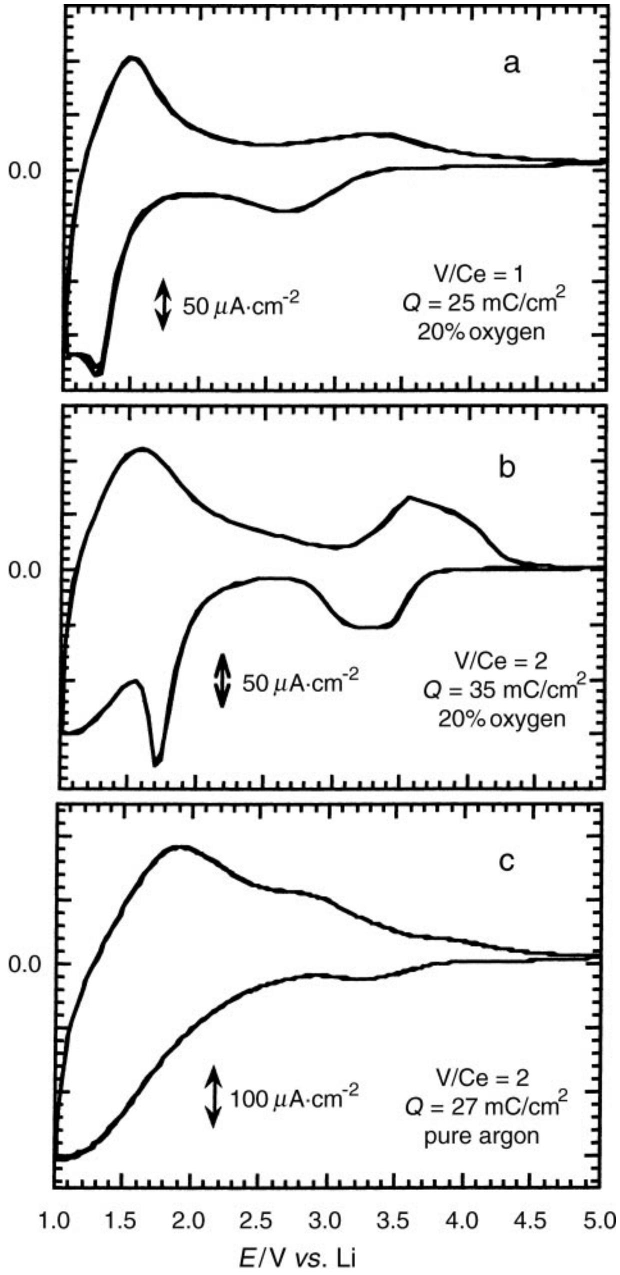

Fig. 1. Cyclic voltammograms of Ce-V mixed oxide films in 1 *M* LiClO4-*PC* anhydrous electrolyte; scan rate: 5 mV/s; a: V/Ce = 1, reactive sputtering with 20% oxygen, thickness 90 nm; b: V/Ce = 2, reactive sputtering with 20% oxygen, thickness 84 nm; c: V/Ce = 2, sputtering in pure argon, thickness 120 nm

[9, 10]. The absence of oxygen in the sputtering atmosphere, on the other hand, produced less crystalline samples and induced the suppression of the redox peaks located at higher potentials in the CV (Fig. 1c), with a corresponding decrease in the intercalated charge.

According to the objectives of this paper, *i.e.* the search for passive electrodes with highest charge capacity, the samples produced with the Ce:V = 1:2 target and with the higher oxygen flow were selected, and only such samples will be described in the following experiments. Formally, from the RBS results, we could write the formula CeV_2O_8 for such samples, but this only reflects the coexistence of different compounds in the same material.

Controlled potential experiments

Cyclic voltammetry was performed on the film electrodes at different scan rates. A linear dependence of the current peak on the scan rate was observed, typical of transport controlled process [15]. The electrochemical behavior of Ce-V mixed oxides during their first intercalation cycles has been already described [16]. Here we want to analyze the electrode response to extensive cycling. In Fig. 2 we report the results of a durability experiment. The film was cycled at a scan rate of 20 mV/s in the potential range of 1–4.5 V *vs.* Li at constant temperature. Every 100 cycles the film was galvanostatically intercalated and de-intercalated, and its *in situ* optical transmittance variation was recorded.

The first cycle (not shown) denoted permanent lithium incorporation (about $5\,mC \cdot cm^{-2}$). However, during the first 70 cycles the electrode underwent an activation process. In fact, the amount of charge inserted/extracted during the potentiodynamic experiment raised from 45 to $48\,mC \cdot cm^{-2}$. Capacity increase has been reported for a series of $LiMVO_4$-based electrodes (M = Cd, Co, Zn, Ni, Cu, Mg) [17]. After 100 cycles, the charge started to decrease stabilizing around $35\,mC \cdot cm^{-2}$ after 200 cycles and $31\,mC \cdot cm^{-2}$ after 300 cycles. However, the charge exchanged under the same conditions during CV was only $16\,mC \cdot cm^{-2}$ after 1000 cycles.

In Fig. 3 the double-logarithmic plot of de-intercalation current *vs.* time for an applied tension of 4 V is shown. In this chronoamperometric experiment the thin

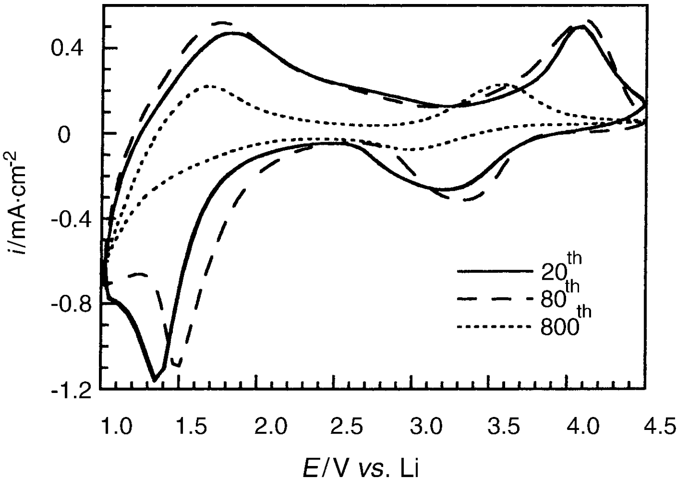

Fig. 2. Cyclic voltammograms of Ce-V mixed oxide film (thickness 78 nm) in 1 *N* $LiClO_4$/*EC-DMC* anhydrous electrolyte; scan rate: 20 mV/s; voltammograms refer to the 20th, 80th, and 800th cycle

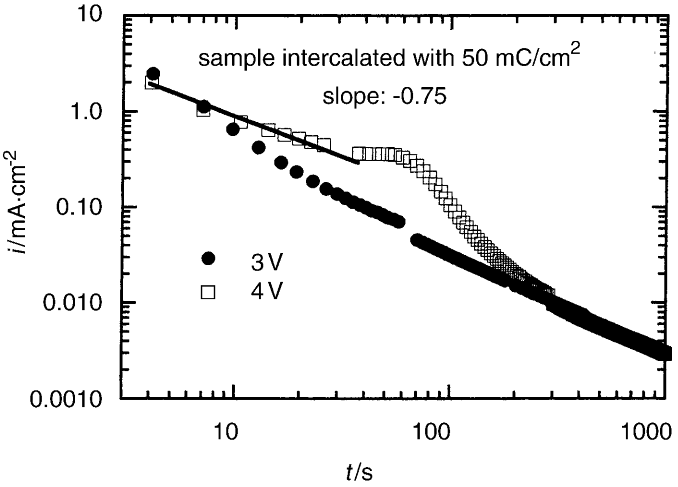

Fig. 3. Double-logarithmic plot for the anodic (lithium de-intercalation) current *vs.* time for Ce-V mixed oxide polarized at 3 and 4 V *vs.* Li; the sample was previously intercalated with 50 mC/cm^2

film has been previously loaded with 50 mC · cm^{-2}. It is evident that there is not a single slope, but a complex decay of the de-insertion current indicating the presence of several mechanisms at different times.

Controlled current experiments

In Fig. 4, the potential variation as a function of time during a galvanostatic intercalation reaction at 50 μA · cm^{-2} is reported. The electrode had been previously conditioned by CV for 100 cycles as described above. The plateaux in this plot appear at electrode potentials corresponding to the peak potentials of the CVs (see markers in Fig. 4). The potential gap separating the two active regions (2.5–4.5 V

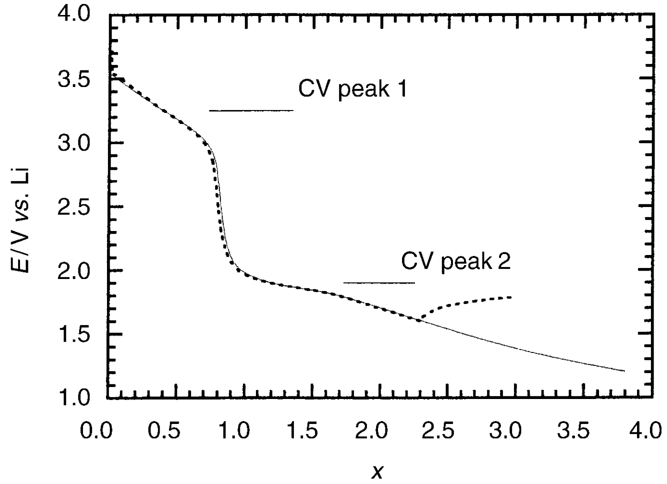

Fig. 4. Cell voltage *vs.* x during a galvanostatic intercalation at 50 μA/cm^2; solid line: deep intercalation up to $x = 4$; dotted line: intercalation up to $x = 2.2$ after several charge-discharge cycles; the markers indicate the peak potentials for Li intercalation in the CVs displayed in Fig. 1b

and 2–1 V) was also clearly visible in the CV. The charge inserted in the range of 3.7–2.5 V corresponds to a lithium molar fraction (referred to vanadium) of $x = 1$. Between 2.5 and 1.5 V, x reached a value of 2.6, and for the fully intercalated sample $x = 4$. It is important to notice that even after charging the electrode up to $x = 4$ the Li charge could be extracted, and a second constant current insertion reaction could then be repeated with reproducible results (Fig. 4, dotted curve).

Short pulses of constant current were also applied to the cell in order to calculate the lithium diffusion coefficient *vs.* lithium concentration by the so-called Galvanostatic Intermittent Titration Technique (GITT). Current density and pulse duration were chosen in a way to fulfill the requirements of the method [18]. The resulting thermodynamic curve *E vs.* Li followed the same behavior as shown in the out-of-equilibrium galvanostatic plot in Fig. 4.

Electrochemical impedance spectroscopy

A preliminary electrochemical impedance spectroscopy (EIS) study has been performed on the thin films at different working electrode potentials, revealing a strong dependence of their EIS response spectra upon Li intercalation. In particular, the high frequency loop was observed to shrink as long as the inserted Li concentration level grew. In Fig. 5, two *Nyquist* plots of the impedance spectra are reported for the electrode at 2.5 V *vs.* Li ($x = 1$). The spectra were recorded during the first intercalation cycle, one taken half-way through towards insertion, the second at the same potential as the first but after partial de-insertion. Due to the irreversible phenomena occurring at the beginning of the intercalation process, some difference between the two spectra could be expected.

The shape of the spectra was typical for an intercalation electrode whose diffusional impedance is rather large. Two regions can be distinguished, a high

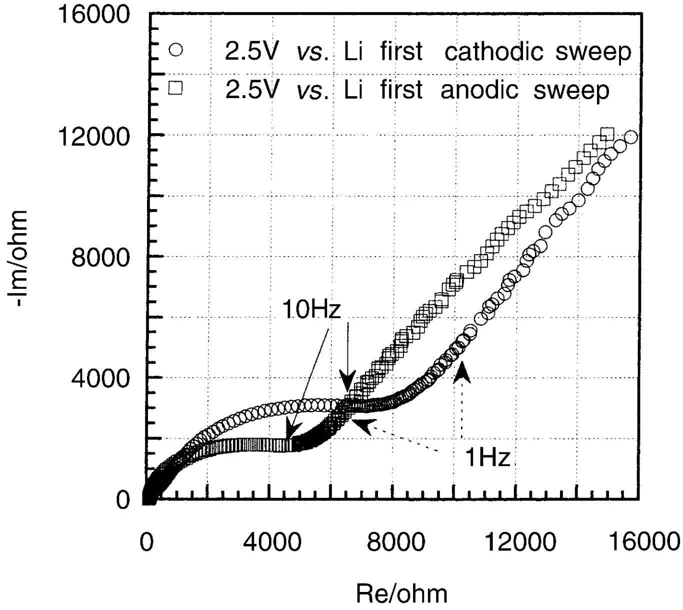

Fig. 5. *Nyquist* plot obtained at 2.5 V *vs.* Li on a Ce-V mixed oxide thin film electrode

frequency region (20 kHz–10 Hz) attributed to charge transfer processes and an intermediate-low frequency region (10–0.05 Hz) of diffusion control. The slope of the diffusional process was the same for both curves, and the finite thickness effect was not detected.

Electrochromism of Ce-V mixed oxide thin films

In Fig. 6 the transmission spectra recorded *in situ* during the galvanostatic insertion performed after 100 and 800 voltammetric cycles are reported. In Fig. 6a the transmission spectrum of the as-deposited film is also shown. Ce-V mixed oxide showed a mixed anodic-cathodic electrochromism as most of the vanadium oxide VO_x films. Upon lithium intercalation (x up to 1) the film bleached as expected for anodically coloring materials. In Fig. 6a the bleaching for wavelengths lower than 450 nm is represented by the shift of the absorption threshold toward shorter wavelengths. However, this shift occurred mainly in the UV part of the spectrum and was therefore barely perceptible to the human eye except during the first intercalation cycles. In fact, lithium intercalation into a pristine sample corresponds to a color variation from yellowish (as-deposited) to transparent. During the de-

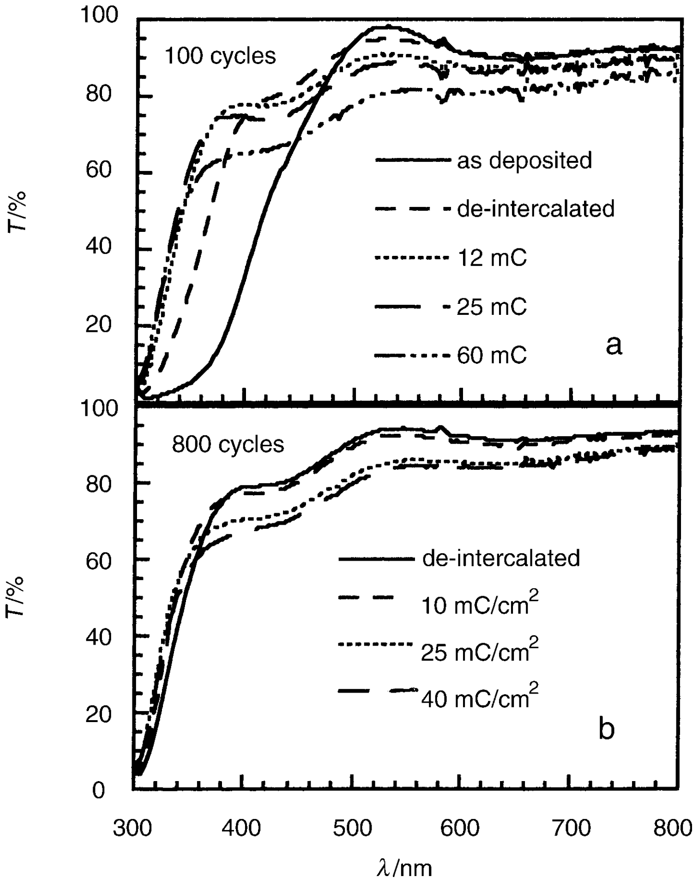

Fig. 6. *In situ* transmittance of Ce-V mixed oxide thin film deposited on ITO after 100 voltammetric cycles (a) and after 800 voltammetric cycles (b); spectra are normalized to cell transmittance

intercalation process the absorption threshold moved back toward the visible region, but it never reached its initial value. This agrees well with permanent lithium incorporation and retention during the first cycles.

Further lithium intercalation (x up to 4) was responsible for a decrease of transmitted light over the whole visible spectrum (cathodic electrochromism). The decrease, however, never exceeded 10% variation. After 800 cycles the anodic electrochromism had almost vanished, and only the weak cathodic transmittance modulation was present.

Evaluation of results

The cerium vanadate reported here is a mixed material containing partly stoichiometric, well-defined crystalline oxides, and an excess of amorphous compounds mainly consisting of vanadium oxides which yield the typical, pale yellowish color to the pristine thin film sample. The electrochemical characterization, however, denotes an electrode behavior very similar to that of wakefieldite (*i.e.* stoichiometric $CeVO_4$), except for the enhanced Li-charge capacity (up to $48\,mC \cdot cm^{-2}$ by CV as compared to $20\,mC \cdot cm^{-2}$ of a $CeVO_4$ film of the same thickness deposited by the sol-gel method [8]). To obtain such a large charge capacity, however, an electrode conditioning of several voltammetric cycles is needed, during which a significant amount of Li is irreversibly inserted and retained inside the film. The charge retained inside the electrode is also larger than the corresponding irreversible charge retained in the more crystalline $CeVO_4$ electrode deposited by the sol-gel process, and is consistent with what has been observed by other authors [19], *i.e.* that the irreversible capacity of the (partially) amorphous orthovanadates is higher than that of the corresponding crystalline compounds. The larger charge capacity discussed above was also confirmed from galvanostatic experiments, where x values up to 4 was obtained at a potential of 1.2 V (compared to $x = 2$ for the $CeVO_4$ sol-gel electrode [8] in a similar electrochemical experiment). This high value of x is not unusual for insertion electrodes for Li batteries made of metal vanadates, both amorphous and crystalline, as already reported in the literature [19].

As far as the de-insertion reaction is concerned, the findings reported in Fig. 3 need some further discussion. When an anodic current is applied to the intercalated electrode, lithium ions are driven away from the electrode across the electrochemical junction, and electrons are collected at the ITO current collector. At the beginning of this process the measured current is the result of several transient processes. Once all other transients become unimportant, several models have been developed to describe the current decay in insertion reaction electrodes. To explain the first part of the de-intercalation process at 4 V we will refer to the model of *Faughnan et al.* proposed for space charge limited (SCL) current [20]. The space charge is formed due to the significant difference in electron and cation mobility. In this model the current is limited by the space charge and decays with $t^{-3/4}$, as indeed observed for our sample (Fig. 3). This model applies to semiconductor electrodes where the electron/cation mobility ratio is significantly greater than one. A change of slope indicates a transition to a different regime, as it was apparent around 100 s in our experiments. We suppose that after the deintercalation of a considerable amount of lithium the material recovered its insulating properties. Then, the anodic current dropped with time more rapidly than before, and the assumptions necessary for the SCL current are no longer valid. Similar SCL de-insertion currents were obtained only for electrode potentials above 3.5 V. We did not expect a SCL current when applying a potential less than 3.5 V, because this potential is in fact too low to build up an electric field at the semiconductor surface.

The above assumptions, consistent with a semiconductor behavior of the (partially de-inserted) sputtered film, have been lately supported by the detection of an anodic photocurrent by the same electrode film when polarized in the same electrolyte at potentials above 3.5 V and illuminated with light of photon energy higher than the optical bandgap of the material. Previously, the corresponding value has been reported to be 2.6 eV [14].

The diffusion coefficient of Li ions (D_{Li^+}) inside the sputtered mixed oxide films has been calculated by various techniques. The first one was GITT, previously used to calculate analogously the Li diffusivity in sol-gel $CeVO_4$ films. The results of such calculations are shown in Fig. 7. It can be observed that the diffusion coefficient decreases from $3 \cdot 10^{-11}\,\mathrm{cm}^2 \cdot \mathrm{s}^{-1}$ ($x = 0$) to $1 \cdot 10^{-13}\,\mathrm{cm}^2 \cdot \mathrm{s}^{-1}$ ($x = 0.9$), which is about one order of magnitude less than that found in the parent crystalline oxide deposited by the sol-gel method, showing a minimum for $x = 0.6$. The minimum in the D *vs.* x curve has also been reported for crystalline $CeVO_4$ [3]; it appears at x values corresponding to the end of the voltammetric peak in the high voltage region (4.5–2.5 V *vs.* Li) or, alternatively, towards the end of the plateau in the galvanostatic discharge. This behavior has been reported by *Aurbach* for Li intercalated graphite electrodes [21]. In this case, the diffusion coefficient had been calculated using the potentiostatic intermittent titration technique (PITT) which is an alternative technique to investigate thermodynamics and mass transport in intercalation electrodes. In the cited paper, an *in situ* – XRD investigation was coupled with kinetic studies, and the minima of the diffusion coefficient were

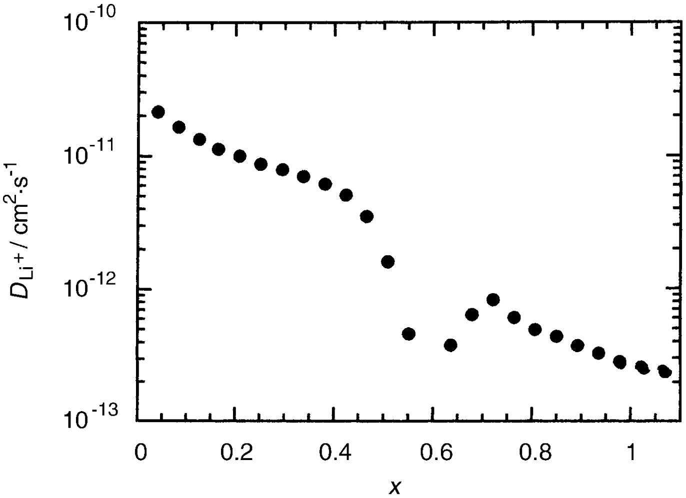

Fig. 7. Li diffusion coefficient as a function of x after intermittent current pulses (GITT); parameters: current density: $100\,\mu\mathrm{A/cm}^2$, pulse duration: 5 s, relaxation time: 3600 s

interpreted in terms of growing of clusters able to trap the diffusing ions at the beginning of a new phase formation.

The origin of this low value for D_{Li^+} is not yet clear taking into account (RBS data) that the sputtered film is less dense than the crystalline material. One possible explanation, presently investigated by XPS of Li-intercalated samples, could be the co-intercalation of solvent molecules with the alkali ion inside the oxide matrix.

Another technique for calculating D_{Li^+} makes use of electrochemical impedance data. Following the paper of *Ho et al.* [22], D_{Li^+} was obtained from the diffusive part in the impedance spectrum (the *Warburg* linear part with a 45° slope) using Eq. (1).

$$|Z| = \left| \frac{V_M(\mathrm{d}E/\mathrm{d}x)}{FD^{1/2}S} \cdot \omega^{-1/2} \right| \tag{1}$$

V_M is the molar volume calculated from the density, dE/dx is the differential of the electrode potential with respect to composition obtained by the coulometric titration for a Li/V elemental ratio of 1, and S is the electrode area. The value of $2.7 \cdot 10^{-13}\,\mathrm{cm}^2 \cdot \mathrm{s}^{-1}$ calculated under such conditions seems to be in good agreement with the data from GITT shown in Fig. 7.

Cerium-vanadium mixed oxide thin films can accommodate a considerable amount of charge without a significant loss of transparency, as already shown by the transmittance data reported in Figs. 6a and 6b. Quantitative data on the electrochromic effect can be obtained considering the optical density (*OD*) variation, where *OD* was defined as usual:

$$OD = \log \frac{T_0}{T_q} \tag{2}$$

Here, T_0 is the initial transmittance and T_q is the measured transmittance after the insertion of the charge q. Many authors have measured the change in transmission at just one wavelength for convenience, but this may lead to wrong values of the optical density because in this way interference effects cannot be eliminated. In order to give a more appropriate description of the transmittance change, the photoptic transmission T was used in the calculation of the optical density, *i.e.* the monochromatic transmittance $T(\lambda)$ was multiplied by a weighting function and integrated over the wavelength range. The weight function used in this case is the eye response spectrum [23].

$$T = \frac{\int T(\lambda) eye(\lambda) \mathrm{d}\lambda}{\int eye(\lambda) \mathrm{d}\lambda} \tag{3}$$

The optical density data reported in Fig. 8 have been calculated from the transmittance spectra $T_q(\lambda)$ shown in Fig. 6. The calculated photoptic transmittance for the as-deposited film is 94%, and that of the cycled sample in its de-intercalated state is only 1% less although the two spectra in Fig 6a look rather different. This is due to the choice of the weight function $eye(\lambda)$ which in our case completely masks every modulation taking place outside the visible range.

Because of such a small difference of photoptic transmittances, the transmittance spectrum of the as-deposited film was used as T_0 in the calculations. Even if the *OD* values reported will be slightly overestimated we prefer to have always the

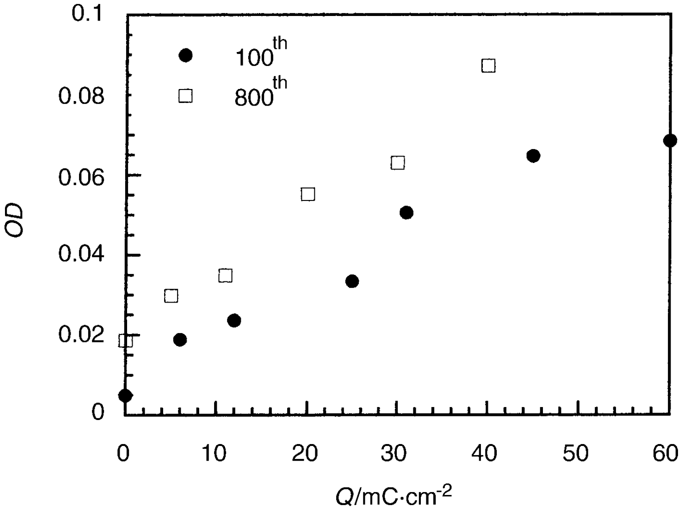

Fig. 8. Optical density as a function of the inserted charge calculated from transmittance spectra recorded after 100 and 800 voltammetric cycles; transmittance values are weighted by the human eye response and integrated over the wavelength range

same reference and follow the evolution of the *OD* during successive cycles. *OD* values are positive and do not vary considerably as a function of the inserted charge (typical of passive materials), never reaching the value of 0.1. This can be compared with 0.7, the value measured for sputtered WO_3 after the insertion of a comparable amount of charge [24].

The coloration efficiency (the slope of the reported graph) was the same for both experiments performed at different times of the electrode lifetime. A saturation effect for high values of inserted charge is seen in the *OD* of the sample cycled 100 times. Because of the sample degradation after 800 CVs it was not possible to insert more than $40\,\mathrm{mC\cdot cm^{-2}}$ during the galvanostatic discharge. This value of charge, however, is rather large compared to the $16\,\mathrm{mC\cdot cm^{-2}}$ inserted during the corresponding 800th voltammogram. We have to hypotize, therefore, that the loss of charge capacity is not as dramatic as it seems from CV measurements, and that the rate of the intercalation reaction, and not the total charge capacity of the electrode, has lowered after extensive cycling.

Conclusions

Ce-V mixed oxides proved to be good counterelectrodes for electrochromic devices. Their rather passive optical behaviour, coupled with a very good charge capacity, ranks them as one of the most promising ion storage materials.

We investigated thin films of different composition and deposited under different conditions. Films of 0.1 μm thickness having the composition V:Ce = 2:1 and deposited in an atmosphere rich of oxygen are able to intercalate $40\,\mathrm{mC\cdot cm^{-2}}$ with an *OD* of 0.05. This rather high charge capacity can be related to the excess of vanadium oxides in the mixed oxide, to the low cristallinity, and to the open morphology of the sputtered films as deduced from X-ray spectroscopy and from the low density of the material. The Li-insertion reaction, after electrode conditioning during several voltammetric cycles, is reversible. Upon extensive cycling there is some worsening of the electrode performance which seems to be related more to kinetic factors than to an effective loss of charge capacity.

Experimental

Thin films of cerium-vanadium mixed oxide have been deposited by RF sputtering using targets made of pressed powders. The targets were prepared by filling a 3 mm deep stainless steel holder of 140 mm diameter with the powder which was previously carefully mixed in the appropriate molar ratio to yield a Ce/V elemental ratio of either 0.5 or 1 for the two targets described henceforth. Afterwards, the targets were compacted with 25 tons at room temperature to reduce the air volume and improve thermal conductivity. No thermal treatment or sintering process was used, and a sputter-up configuration of the sputtering system was adopted. To avoid sputtering of the target holder, a properly designed ground shield was used to inhibit the discharge of the external side of the target itself. The effectively sputtered area has a diameter of 130 mm.

Cerium-vanadium mixed oxide targets were sputtered in a reactive atmosphere at a total pressure of 30 mtorr with the oxygen pressure varying from zero up to 5 mtorr; the RF power applied was 150 W. A long pre-sputtering time was required when the target was inserted in the sputtering chamber for the first time. In fact, due to the extended real surface area of pressed powders (compared to sintered targets), the degassing process could take a long time; it was monitored following the pressure in the chamber. Moreover, this long pre-sputtering procedure allowed the surface of the target to reach a stationary concentration of species, thus compensating for different sputtering yields. X-Ray diffraction patterns of the sputtered films revealed the presence of $CeVO_4$-W (*i.e.* wakefieldite) together with amorphous VO_x for samples deposited at high oxygen concentration. Films deposited in an oxygen-free atmosphere were amorphous.

Electrochemical experiments were performed using a three-electrode cell with lithium metal foils serving as counter and reference electrodes. $LiClO_4$ in PC (Propylene carbonate) was used as organic electrolyte, and the cell was assembled in an argon filled dry-box.

Thin film transmittance variation was measured *in situ* as a function of the inserted charge using a Perkin Elmer λ-19 spectrophotometer. The electrochemical cell used for this kind of measurements was provided with flat windows mounted for experiments at normal incidence of light. All reported spectra were normalized to the transmittance of the cell filled with the electrolyte without any electrode in the beam path. *Ex situ* film transmittance and reflectance measurements have been reported elsewhere [14]. From such measurements, thin film refractive index and thickness (120 nm; double-checked by standard profilometry) have been evaluated.

The film density was calculated from its thickness on the basis of RBS (*Rutherford* backscattering) measurements from which the concentration of oxygen, cerium, and vanadium can be determined as well. A value of $3.46\,g \cdot cm^{-3}$ ($4.3\,g \cdot cm^{-3}$) was obtained for the mixed oxide film from the target with a Ce/V ratio of 0.5 (1.0) sputtered in an atmosphere containing 20% of oxygen. These values can be compared with 7.13 and $3.35\,g \cdot cm^{-3}$ reported for crystalline CeO_2 and V_2O_5 and with $4.76\,g \cdot cm^{-3}$ of wakefieldite [13].

The molar fraction of lithium inside the film was calculated from the inserted charge and referred to vanadium concentration. In all experiments it was assumed that vanadium is the only electrochemical active species, *i.e.* that any change in oxidation state due to Li insertion occurs only with vanadium atoms. XPS measurements confirmed that cerium is always present in its lower oxidation state (3+), even before any Li insertion experiment has been undertaken.

Acknowledgments

This work was partially financed by the *Consiglio Nazionale per le Ricerche* (CNR) in the frame of the project MSTA2 under the contract 98.00045.PF34 and by the ministry MURST, *Cofinanziamento*

1999. We thank *M.-C. Hugon* for RBS measurements and *S. Magnifico*, *F. Artuso*, *F. Bonino*, and *F. Croce* for useful discussions.

References

[1] Granqvist CG (1995) Handbook of Inorganic Electrochromic Materials. Elsevier, Amsterdam
[2] Baudry P, Rodrigues ACM, Aegerter AM, Bulhoes LO (1990) J Non-Cryst Solids **121**: 319
[3] Kéomany D, Petit J-P, Deroo D (1994) Proc SPIE **2255**: 363
[4] Stromme Mattsson M, Azens A, Niklasson GA, Granqvist CG (1997) J Appl Phys **81**: 6432
[5] Talledo A, Granqvist CG (1994) J Phys D Appl Phys **27**: 2445
[6] Hutchins MG, Butt NS, Ageorges P (1999) Electrochimica Acta **44**: 3271
[7] Cogan SF, Rauh RD, Nguyen NM, Plante TD, Westwood JD (1993) J Electrochem Soc **140**: 112
[8] Picardi G, Varsano F, Decker F, Opara-Krasovec U, Surca A, Orel B (1999) Electrochim Acta **44**: 3157
[9] Opara-Krasovec U, Orel B, Surca A, Bukovec N, Reisfeld R (1999) Solid State Ionics **118**: 195
[10] Opara-Krasovec U, Orel B, Reisfeld R (1998) Electrochem Solid-State Lett **1**: 104
[11] Bange K (1999) Sol Energy Mater Sol Cell **58**: 131
[12] Masetti E, Varsano F, Decker F (1999) Electrochim Acta **44**: 3117
[13] Baudracco-Gritti C, Quartieri C, Vezzalini G, Permingeat F, Pillard F, Rinaldi R (1987) Bull Mineral **110**: 657
[14] Varsano F, Krasilnikova A, Decker F, Masetti E (1999) SPIE Proceedings, vol 3738. Berlin, p 97
[15] Hitchman ML (1979) Thin Solid Films **61**: 341
[16] Varsano F, Decker F, Masetti E (1999) Ionics **5**: 80
[17] Sigala C, Guyomard D, Piffard Y, Tournoux M (1995) CR Acad Sci Paris **320** (IIb): 523
[18] Weppner W, Huggins RA (1977) J Electrochem Soc **124**: 1569
[19] Denis S, Baudrin E, Touboul M, Tarascon JM (1997) J Electrochem Soc **144**: 4099
[20] Faughnan BW, Crandall RS, Lampert MA (1975) Appl Phys Lett **27**: 275
[21] Levi MD, Levi EA, Aurbach D (1997) J Electroanal Chem **421**: 89
[22] Ho C, Raistrick ID, Huggins RA (1980) J Electrochem Soc **127**: 343
[23] Burdis MS, Siddle JR (1994) Thin Solid Films **237**: 320
[24] Varsano F (1999) PhD Thesis

Received June 23, 2000. Accepted (revised) August 7, 2000